Reevaluation of the role of the Pam18:Pam16 interaction in translocation of proteins by the mitochondrial Hsp70-based import motor

June E. Pais, Brenda Schilke, and Elizabeth A. Craig
Department of Biochemistry, University of Wisconsin–Madison, Madison, WI 53706

ABSTRACT The heat-shock protein 70 (Hsp70)–based import motor, associated with the translocon on the matrix side of the mitochondrial inner membrane, drives translocation of proteins via cycles of binding and release. Stimulation of Hsp70's ATPase activity by the translocon-associated J-protein Pam18 is critical for this process. Pam18 forms a heterodimer with the structurally related protein Pam16, via their J-type domains. This interaction has been proposed to perform a critical regulatory function, inhibiting the ATPase stimulatory activity of Pam18. Using biochemical and genetic assays, we tested this hypothesis by assessing the in vivo function of Pam18 variants having altered abilities to stimulate Hsp70's ATPase activity. The observed pattern of genetic interactions was opposite from that predicted if the heterodimer serves an inhibitory function; instead the pattern was consistent with that of mutations known to cause reduction in the stability of the heterodimer. Analysis of a previously uncharacterized region of Pam16 revealed its requirement for formation of an active Pam18:Pam16 complex able to stimulate Hsp70's ATPase activity. Together, our data are consistent with the idea that Pam18 and Pam16 form a stable heterodimer and that the critical role of the Pam18:Pam16 interaction is the physical tethering of Pam18 to the translocon via its interaction with Pam16.

INTRODUCTION

The mitochondrial matrix, the site of numerous important metabolic processes, contains hundreds of different proteins. All but a handful are encoded by nuclear DNA and synthesized on cytosolic ribosomes. Thus efficient translocation of these proteins across the mitochondrial membranes is critical. Typically, such proteins are synthesized with a positively charged N-terminal targeting presequence, which is first recognized by receptors on the outer membrane and then transferred sequentially through proteinaceous channels in the outer and inner membranes, formed by components of the TOM and TIM23 complexes, respectively. The movement of the presequence through the Tim23 channel is strictly dependent on a mem-

brane potential across the inner membrane. However, the translocation of the remainder of the protein requires the action of the heat-shock protein 70 (Hsp70)–based, presequence translocase-associated motor complex (PAM), which resides on the matrix side of the inner membrane (Jensen and Johnson, 2001; Neupert and Brunner, 2002; Koehler, 2004; Rehling et al., 2004; Wiedemann et al., 2004; Neupert and Herrmann, 2007).

The core component of PAM is the matrix Hsp70, called Ssc1 in yeast. Ssc1 is tethered to the translocon by another component of the motor complex, Tim44 (Rassow et al., 1994; Schneider et al., 1994). Like all Hsp70s, Ssc1, in its ATP-bound state, rapidly binds exposed hydrophobic stretches of its client protein. For the Hsp70-based PAM motor to provide the driving force of the movement of the polypeptide across the membrane, stabilization of the interaction of Ssc1 with the translocating polypeptide is critical. This interaction is very transient, with stabilization depending upon hydrolysis of the bound ATP. However, although Hsp70s have an intrinsic ATPase activity, the basal rate is very low; stimulation by a partner J-protein is required to stabilize client protein interaction. All J-proteins contain an ~60–amino acid J-domain, which directly interacts with Hsp70 to effect this stimulation. Predominantly α-helical, J-domains have a conserved fold, with the major helices, 2 and 3, having
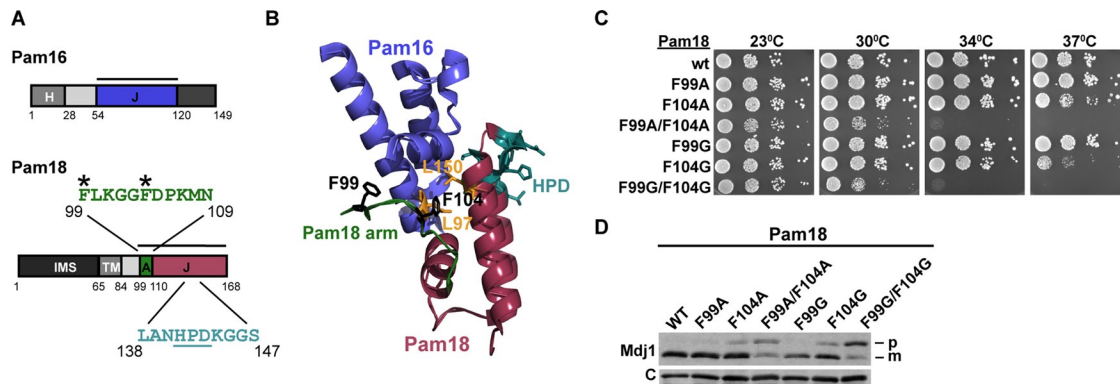
FIGURE 1: Characterization of the Pam18 "arm." (A) Schematic representation of Pam16 and Pam18. Pam16: amino acids (aa) 1–27, hydrophobic (H); aa 54–119, J-like domain (J). Pam18: aa 1–60, intermembrane space (IMS); aa 65–83, transmembrane (TM); aa 99–109, arm (A); aa 110–168, J-domain (J). Sequences shown: the arm with the critical residues F99 and F104 indicated by an asterisk; the HPD (underlined) and surrounding residues of the J-domain. Segments used in structural determination (Mokranjac et al., 2006) are indicated by the solid black lines. (B) Structure of Pam18 (aa 99–168, pink) complexed with Pam16 (aa 54–119, blue) (Mokranjac et al., 2006; PDB ID 2GUZ). The residues examined in this study are highlighted as follows, with individual residues shown as ball-and-stick models: Pam18 arm aa 99–109, green; Pam18$_{F99}$ and Pam18$_{104}$, black; Pam18 HPD-region residues 138–147, teal; Pam18$_{L150}$ and Pam16$_{L97}$ at the heterodimer interface, orange. (C) Growth phenotypes of mutants expressing variants with alterations in the arm of Pam18. Tenfold serial dilutions of pam18-Δ cells carrying a plasmid expressing either wt or indicated PAM18 mutant gene were spotted onto rich glucose-based media, followed by incubation at the indicated temperatures for 2 d (30, 34, and 37°C) or 4 d (23°C). (D) In vivo accumulation of Mdj1 precursor in cells expressing Pam18 arm variants. pam18-Δ cells carrying a plasmid expressing either wt PAM18 or indicated mutant gene were grown in rich media at a permissive temperature (23°C) to early log phase and then shifted to 37°C and grown for 4–6 h to induce the phenotype. Whole-cell lysates were analyzed by SDS–PAGE and immunoblotting using Mdj1- and, as a control (C), Ssc1-specific antibodies. m, mature form of Mdj1; p, precursor form of Mdj1.

an extended loop with an invariant HPD motif, which is critical for stimulation (Bukau et al., 2006; Craig et al., 2006).

In the case of the import motor, Pam18 (also known as Tim14), a translocon-associated transmembrane protein, is the J-protein partner of Ssc1 (D'Silva et al., 2003; Mokranjac et al., 2003; Truscott et al., 2003). Pam18, a 168–amino acid protein, has, in addition to a C-terminal matrix-localized J-domain, a single membrane-spanning region and an N-terminal domain in the intermembrane space (IMS) (Figure 1A). This IMS domain interacts with Tim17, as well as Tim23, a core component of the translocon itself, and stabilizes Pam18's association with the translocon (D'Silva et al., 2003, 2008; Truscott et al., 2003; Chacinska et al., 2005; Tamura et al., 2009). In addition, Pam18's J-domain interacts with Pam16 (also called Tim16), a 149–amino acid protein whose N-terminus associates with the translocon, probably indirectly, via interaction with Tim44 (Figure 1A; Frazier et al., 2004; Kozany et al., 2004; Mokranjac et al., 2007; D'Silva et al., 2008; Hutu et al., 2008). Thus Pam18's association with the translocon is multifaceted via direct interactions in the IMS and indirect interactions in the matrix.

Pam16 contains a "J-like domain." Although this has structural and sequence similarity to the J-domain of Pam18, it is not capable of stimulating the ATPase activity of Ssc1 (Li et al., 2004; D'Silva et al., 2005b). Pam18 and Pam16 interact via their J- and J-like domains to form a stable heterodimer, which is critical for protein translocation and cell viability (Truscott et al., 2003; D'Silva et al., 2005b, 2008). A high-resolution structure of a complex between a 69–amino acid fragment of Pam18 and a 65–amino acid fragment of Pam16 (amino acids 99–168 and 54–149, respectively) containing these J-type domains has been determined (Mokranjac et al., 2006). The heterodimeric complex has a pseudosymmetrical arrangement (Figure 1B), with the helices and the intervening loop between the J-type domains tightly packed. In addition, the Pam18 fragment includes

10 amino acids N-terminal to the J-domain, which form an "arm" that wraps around Pam16's J-like domain (Figure 1B). This Pam18$_{99-168}$:Pam16$_{54-149}$ complex is unable to stimulate Ssc1's ATPase activity and has been proposed to represent an inhibited conformation (Mokranjac et al., 2006).

An unresolved question concerns the function(s) of the interaction between Pam16 and Pam18 in vivo. It is known that Pam16 plays an important role in tethering Pam18 to the translocon (D'Silva et al., 2005b, 2008). It has also been proposed, and generally accepted, that the interaction between the J-domain of Pam18 and the J-like domain of Pam16 is dynamic and serves a critical role in regulating the ability of Pam18 to stimulate the ATPase activity of Hsp70 (Frazier et al., 2004; Mokranjac et al., 2006; Mokranjac and Neupert, 2010; van der Laan et al., 2010; Endo et al., 2011). According to this model, regulation is imposed by altering the conformation of the Pam16:Pam18 interface, relieving the type of inhibitory structural constraints observed in the structure described earlier, and thus allowing stimulation of Hsp70's ATPase activity. The Pam18 arm is proposed to play a critical role, based on the analysis of variants having alterations in the arm and on the inactivity of the heterodimer containing truncated Pam16 (Mokranjac et al., 2006). The idea that the interaction between the two J-type domains serves a regulatory role is an intriguing one. Such regulation could provide a means of specifically activating the motor when a translocating polypeptide has engaged at the translocon, as unregulated stimulation would cause a futile cycle of ATP hydrolysis, ADP release, and ATP rebinding even when not needed for client interaction. Therefore we decided to further investigate the interaction between Pam18 and Pam16, testing this model of regulation using genetic and biochemical approaches. The results of our studies provide no evidence for regulation of the activity of the Pam18:Pam16 heterodimer via modulation of the interface of the two proteins. Instead

our results support the critical importance of the interaction, not only of the J-domains themselves, but also of the adjacent N-terminal residues of Pam16 and Pam18 in stabilization of the heterodimer and thus Pam18's association with the translocon.

RESULTS

Functional importance of residues in the arm and the HPD regions of Pam18

If the interaction of Pam18 with Pam16 serves to inhibit its ATPase stimulatory ability until needed to facilitate Ssc1's interaction with a client protein, it is reasonable to posit that 1) an increase in Pam18's stimulatory ability would be deleterious when such inhibition is compromised and 2) a decrease in stimulatory ability might be advantageous under such circumstances. To obtain the tools to test these predictions, we first created two series of mutants encoding alterations in Pam18. First, using site-directed mutagenesis, we individually changed each codon for the Pam18 arm (amino acids 99–109; Figure 1) to an alanine codon to determine which residues of the arm were functionally most important. Second, we isolated a series of mutations altering residues in and near the invariant HPD motif, with a goal of identifying variants having ATPase stimulatory activity either higher or lower than that of wild-type (wt) Pam18.

Centromeric plasmids carrying genes encoding single–amino acid substitutions in the arm of Pam18 were transformed into a $pam18$-Δ strain carrying wt $PAM18$ on a plasmid that also contained the $URA3$ gene. By streaking resulting transformants on plates containing 5-fluoroorotic acid (5-FOA), we selected those cells having lost the plasmid carrying the wt $PAM18$ gene and then tested them for growth at a variety of temperatures. We also included the double mutant $pam18_{F99G/F104G}$ in our analysis, as it was analyzed in an earlier study and proposed to be critical for regulation (Mokranjac et al., 2006). As previously reported, $pam18_{F99G/F104G}$ cells have a strong temperature-sensitive phenotype, growing extremely poorly above 30°C (Figure 1C). On the other hand, the only single-alanine substitution that showed a phenotype was $pam18_{F104A}$, which was only slightly temperature sensitive at 37°C (Figure 1C). All of the other mutants having single-alanine substitutions in the arm, including $pam18_{F99A}$, grew as well as wt (Figure 1C and Supplemental Figure S1). Several double-alanine mutants were also constructed, using the available structural information to concentrate on those amino acids whose side chains faced Pam16 (Mokranjac et al., 2006). Of the mutants tested ($pam18_{F99A/F104A}$, $pam18_{F99A/L100A}$, $pam18_{K101A/K107A}$, $pam18_{G102A/G103A}$, $pam18_{F104A/F149A}$, $pam18_{D105A/P106A}$, and $pam18_{M108A/N109A}$), none had an obvious growth defect, other than $pam18_{F99A/F104A}$ (Figure 1C and Supplemental Figure S2). $pam18_{F99A/F104A}$ grew slightly better than $pam18_{F99G/F104G}$ at 30°C but grew as poorly at temperatures above 30°C (Figure 1C). We then constructed single-glycine substitution mutations at residues F99 and F104. $pam18_{F99G}$ grew as well as wt; however, $pam18_{F104G}$ grew poorly at 37°C, with a stronger phenotype than $pam18_{F104A}$. These variants were expressed at normal levels (Supplemental Figure S3A), indicating that the phenotypes observed were not due to protein instability.

Many mitochondrial proteins contain an N-terminal targeting presequence that is cleaved after translocation to the mitochondrial matrix. A defect in mitochondrial import therefore can be detected by monitoring the accumulation of the precursor form of a mitochondrial protein. To demonstrate that the growth phenotypes of the $PAM18$ mutants correlate with defects in mitochondrial import, the accumulation of the precursor form of Mdj1, a nuclear-encoded mitochondrial protein, was monitored for each of the strains tested,

using immunoblot analysis (Figure 1D). Cells were first grown at 23°C, then shifted to 37°C and grown for 4–6 h to induce the phenotype. The magnitude of the precursor accumulation correlated with the severity of the growth phenotypes. Wild-type, as well as $pam18_{F99A}$ and $pam18_{F99G}$, cells showed negligible amounts of nonprocessed Mdj1 precursor (Figure 1D). $pam18_{F104A}$ and $pam18_{F104G}$ had modest accumulation, whereas the majority of Mdj1 in the double mutant $pam18_{F99A/F104A}$ was in the precursor form. The greatest amount of precursor accumulation was observed for $pam18_{F99G/F104G}$. Together these results suggest that residue 104 is arguably the most important residue of the arm. However, no residue plays a critical role, as each can individually be changed to alanine with very little phenotypic effect. For further analysis we used $pam18_{F99G/F104G}$ because this mutant exhibited the strongest phenotype and to make our results most comparable to previously published data (Mokranjac et al., 2006).

To identify a set of Pam18 variants that altered ATPase stimulatory ability, we constructed 15 mutations that caused alterations in seven residues near and around the invariant HPD motif (Figure 1). The effect of these alterations on the ability of Pam18 to stimulate Ssc1's ATPase activity in vitro and to function in vivo was tested, searching for variants that had altered activity but allowed growth of $pam18$-Δ cells. To assess their ability to substitute for wt Pam18, we used the plasmid-shuffling approach described earlier. To measure Hsp70 stimulation we used an Ssc1 variant having a single amino acid alteration in the substrate-binding cleft, V459F, in order to ensure that the stimulation measured was the result of J-domain interaction and not of any inadvertent binding of hydrophobic sequences in the client protein-binding cleft, which also can cause ATPase activation (Laufen et al., 1999; Mayer et al., 2000). Similar to the analogous, previously characterized DnaK variant (Mayer et al., 2000), $Ssc1_{V459F}$ had a normal basal ATPase activity, but it was only negligibly stimulated by client peptide (data not shown).

Of the 15 single–amino acid Pam18 variants generated, 8 supported growth as well as wt (Supplemental Table S1). We chose 5 for further characterization: L138K, N140Q, P142G, K144R, and S147G. Both single turnover, using preformed ^{32}P-ATP complexes, and steady-state assays were used to compare the ATPase stimulatory ability of the variants with that of wt protein. Under both assay conditions, these 5 variants had altered ATPase stimulatory activity (Figure 2A) but allowed cells to grow indistinguishably from those expressing wt Pam18 (Figure 2B). One variant, $Pam18_{K144R}$, had slightly higher activity than wt Pam18, for example, stimulating 9.3-fold compared with 8.0-fold at Pam18 concentrations in 25-fold excess over Ssc1 under single-turnover conditions. The other 4 had reduced activity. The activities of $Pam18_{L138K}$ and $Pam18_{N140Q}$ were moderately reduced, for example, having ~50 and 25% of the activity of wt Pam18, respectively, at Pam18 concentrations in 25-fold excess over Ssc1 under single-turnover conditions. $Pam18_{S147G}$ and $Pam18_{P142G}$ exhibited minimal activity under both assay conditions (Figure 2A). Thus significantly lower ATPase stimulatory activity is well tolerated in vivo.

Low stimulatory activity of Pam18 is deleterious when Pam18's arm is altered

Having the necessary tools in hand, we next assessed the effect of the amino acid alterations that altered ATPase stimulation in the context of the alterations of F99/F104, the residues proposed to be critical for the ability of Pam16 to negatively regulate Pam18's stimulatory activity (Mokranjac et al., 2006). Thus we constructed mutant $PAM18$ genes that encoded variants having three amino acid changes: one of the five alterations in or near the HPD that affect
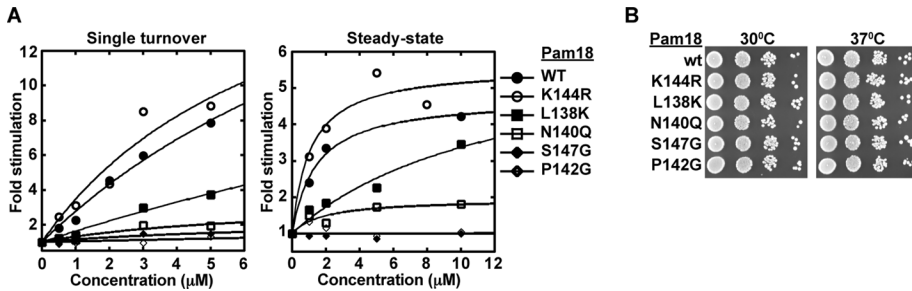
FIGURE 2: Effect of alteration of selected residues in and around the HPD region of Pam18. (A) Stimulation of Ssc1 ATPase activity under single-turnover (left) and steady-state (right) conditions. Reactions contained preformed 0.2 μM Ssc1:[α-³²P]ATP complex (for single-turnover experiments) or 1 μM Ssc1, 12.5 μM ATP, and 2 μM Mge1 (for steady-state experiments) and various concentrations of Pam18 as indicated. Reactions were incubated at 25°C for various times, and the rate constants for ATP hydrolysis, determined as described in *Materials and Methods*, are plotted as the fold stimulation over the basal rate determined in the absence of Pam18 (set at 1) versus the concentration of Pam18. The data are fitted to a hyperbolic curve function. (B) Growth phenotypes of cells expressing the Pam18 variants analyzed in A. Tenfold serial dilutions of *pam18-Δ* cells carrying a plasmid expressing either wt or indicated *PAM18* mutant gene were spotted onto rich glucose-based media, followed by incubation at the indicated temperatures for 2 d.

ATPase activity (Figure 2) and the two arm alterations, F99G and F104G. We then tested their ability to support growth of *pam18-Δ* cells, using the *pam18-Δ* plasmid-shuffling strain. Three of the triple mutants were unable to support growth, as no 5-FOA–resistant colonies were obtained, indicating synthetic lethality (Figure 3A). These residues in or near the HPD resulting in synthetic lethality with F99G/F104G were N140Q, S147G, and P142G, all of which caused a reduction in Pam18's ATPase stimulatory activity (Figure 2A). The other two triple mutants yielded viable cells. One, having the L138K alteration, which reduced ATPase stimulatory activity slightly, had no synthetic genetic effect with the F99G/F104G alterations; *pam18F99G/F104G/L138K* cells grew as well as *pam18F99G/F104G* cells. The fifth variant, having the K144R alteration, which slightly increased activity, partially suppressed the growth defect caused by F99G/F104G; *pam18F99G/F104G/K144R* cells grew slightly better than *pam18F99G/F104G* cells, despite having similar expression levels of Pam18 (Figure 3A and Supplemental Figure S3B). We also assessed Mdj1 precursor accumulation in these cells. Consistent with the growth phenotypes, Mdj1 precursor accumulated at similar levels in *pam18F99G/F104G* and *pam18F99G/F104G/L138K* cells but to a slightly

lesser degree in *pam18F99G/F104G/K144R* cells (Figure 3B). In sum, several alterations in Pam18 that decreased stimulatory activity of Pam18 were deleterious when combined with the alterations in the arm, whereas the alteration that enhanced stimulatory ability partially suppressed the growth and import defects caused by the arm alterations.

Alterations of the Pam18 arm, IMS domain, and J domain:J-domain interface have similar effects on function

The severe synthetic growth defects caused by combination of alterations in the arm and HPD region suggested to us that the arm might play an important role in stabilizing the interaction of Pam18 with Pam16 and thus Pam18's interaction with the translocon. To test this idea, we decided to assess the effect of HPD alterations when in combination with mutations previously shown to decrease the stability of Pam18's interaction with the translocon. Our goal was to determine whether they showed the same or a different pattern of genetic interactions as the mutations causing alterations in Pam18's arm. We choose two mutations for analysis: *pam16L97W* and *pam18Δ1-60*. L97 of Pam16 is in the J-type domain and directly contacts Pam18's J-domain (Figure 1B); alteration of this leucine to a tryptophan destabilizes the Pam18:Pam16 interaction (D'Silva et al., 2008). Like *pam18F99G/F104G* cells, *pam16L97W* cells are temperature sensitive for growth and do not form colonies at 37°C (Figure 4A). However, the L97W mutation causes a slightly less severe growth defect. Although *pam16L97W* grew as well as wt cells at 30°C, growth of *pam18F99G/F104G* was slightly impaired at this temperature (Table 1). Pam18Δ1-60 was chosen because its phenotypic consequences are independent of possible confounding effects in the matrix, as it does not lack any matrix localized residues but, instead, only the IMS domain. Under typical laboratory conditions, *pam18Δ1-60* grows indistinguishably from wt cells (Figure 4A; Mokranjac et al., 2007; D'Silva et al., 2008), although it is synthetically lethal with the *pam16L97W* mutation (Supplemental Figure S4), as expected of a mutation that affects the stability of the interaction of Pam18 with the translocon.

The *pam16L97W* and the *pam18Δ1-60* mutations had the same pattern of interactions with the HPD region mutations as the *pam18F99G/F104G* mutation, becoming more severe with greater effects on ATPase stimulation (Table 1). *pam16L97W* had no genetic interaction with K144R but was synthetically lethal with P142G and S147G (Figure 4B). L138K and N140Q had intermediate effects; *pam16L97W pam18L138K* cells had impaired growth at 34°C, whereas *pam16L97W pam18N140Q* cells only grew at 23°C (Figure 4B). As was the case with *pam18F99G/F104G* and *pam16L97W*, *pam18Δ1-60* was synthetically lethal with P142G. In addition, *pam18Δ1-60/S147G* was temperature sensitive, unable to form colonies at 34°C, and *pam18Δ1-60/N140Q* grew very poorly at 34°C (Figure 4C). However, *pam18Δ1-60/K144R*
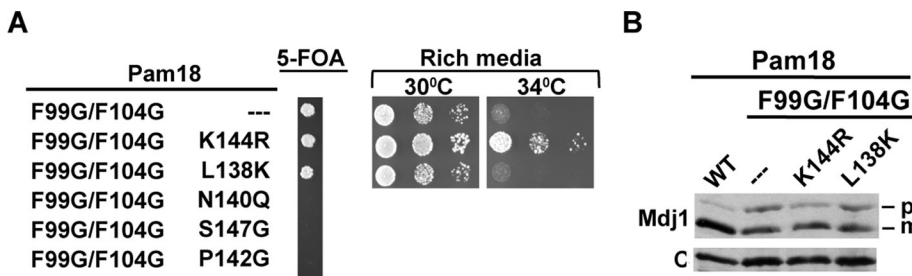

FIGURE 3: Analysis of *PAM18* mutations encoding alterations in the HPD region and the arm. (A) Growth phenotypes of cells expressing the indicated *PAM18* mutant or wild-type *PAM18* gene. Cells were spotted onto plates containing 5-FOA and incubated at 23°C for 4 d. Cells recovered from 5-FOA plates were then spotted in 10-fold serial dilutions onto rich glucose-based media and incubated for 2 d at 30°C or 34°C. (B) In vivo precursor accumulation in cells expressing the Pam18 variants analyzed in A. Cells were grown in rich media at a permissive temperature (23°C) to early log phase and then shifted to 37°C and incubated for 4–6 h to induce the phenotype. Whole-cell lysates were analyzed by SDS–PAGE and immunoblotting using Mdj1- and, as a control (C), Ssc1-specific antibodies. m, mature form of Mdj1; p, precursor form of Mdj1.
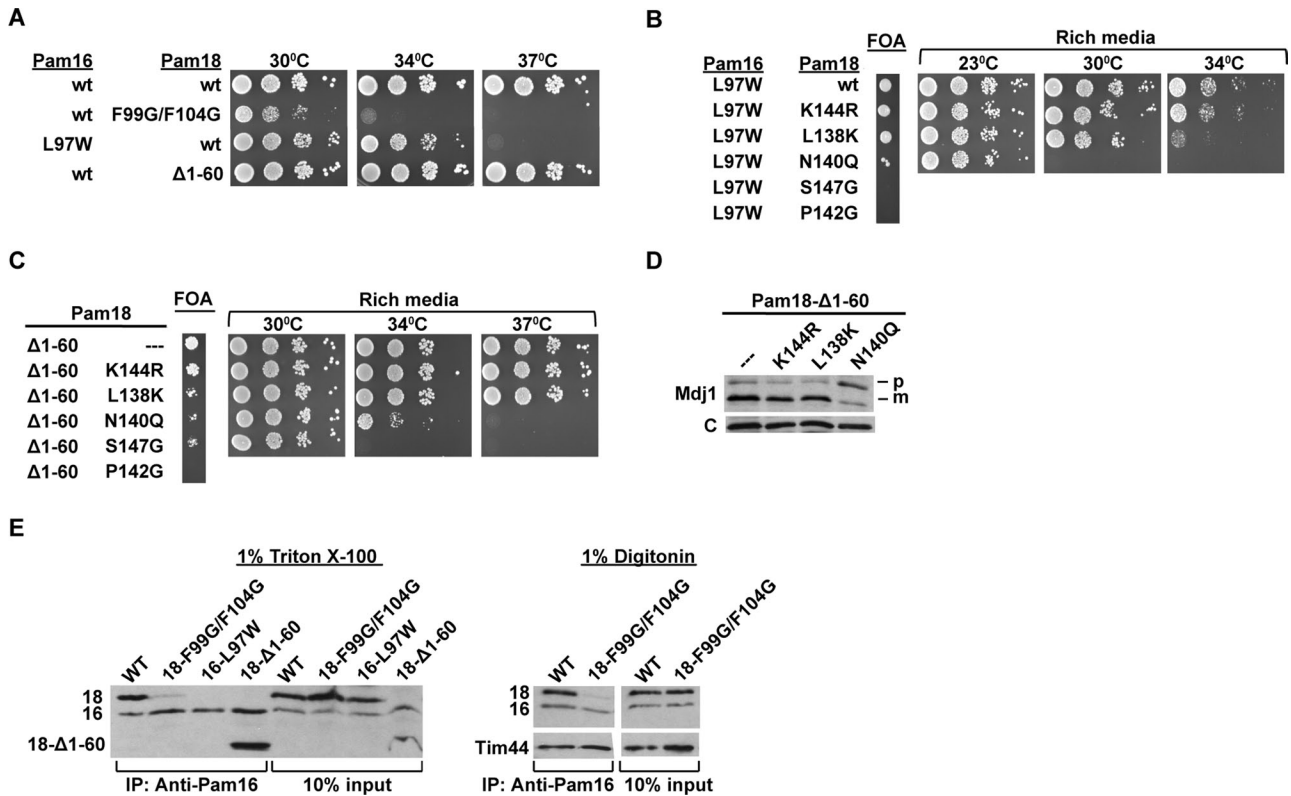
FIGURE 4: Analysis of *PAM18* mutants in the HPD region and mutants that disrupt the stability of the Pam18:Pam16 heterodimer. (A–C) Growth phenotypes of selected mutants. Strains expressing the indicated plasmid-encoded mutant and wild-type *PAM18* and/or *PAM16* genes were plated onto 5-FOA–containing media and incubated at 23°C for 4 d. Strains recovered from plating on 5-FOA were then spotted in 10-fold serial dilutions onto rich glucose-based media and incubated for 2 d (30, 34, and 37°C) or 3 d (23°C). (D) In vivo precursor accumulation in selected mutant strains. Cells were grown in rich media at a permissive temperature (23°C) to early log phase and then shifted to 37°C and grown for 4–6 h to induce the phenotype. Whole-cell lysates were analyzed by SDS–PAGE and immunoblotting using Mdj1- and, as a control (C), Ssc1-specific antibodies. m, mature form of Mdj1; p, precursor form of Mdj1. (E) Coimmunoprecipitation from mitochondrial lysates. Mitochondria were incubated in 1% Triton X-100 or 1% digitonin and then subjected to immunoprecipitation by using Pam16-specific antibodies, followed by SDS–PAGE and immunoblotting against Tim44-, Pam16-, and Pam18-specific antibodies. Ten percent of soluble material after lysis was used as a loading control (10% input).

and $pam18_{\Delta 1\text{-}60/L138K}$ grew like wt at all temperatures tested. The effect of these mutations on in vivo precursor accumulation was also investigated, concentrating on $pam18_{\Delta 1\text{-}60}$ because it causes no obvious growth defect. $pam18_{\Delta 1\text{-}60}$, $pam18_{\Delta 1\text{-}60/K144R}$, and

$pam18_{\Delta 1\text{-}60/L138K}$ accumulated a modest amount of precursor; the precursor level was substantially higher in extracts of $pam18_{\Delta 1\text{-}60/N140Q}$ (Figure 4D). The levels of expression of Pam18 in $pam16_{L97W}$ $pam18_{L138K}$, $pam16_{L97W}$ $pam18_{N140Q}$, and

	PAM18 HPD mutation					
PAM18/16 mutation	None	K144R	L138K	N140Q	S147G	P142G
$pam18_{F99G/F104G}$	TS (30)	TS (34)	TS (30)	Lethal	Lethal	Lethal
$pam16_{L97W}$	TS (34)	TS (34)	TS (34)	TS (30)	Lethal	Lethal
$pam18_{\Delta 1\text{-}60}$	wt	wt	wt	TS (34)	TS (34)	Lethal
$pam16_{51\text{-}53AAA}$	wt	wt	wt	TS (34)	TS (34)	TS (30)
$pam16_{48\text{-}50AAA}$	wt	wt	wt	wt	wt	TS (37)

Summary of in vivo growth phenotypes for *PAM18* and *PAM16* mutants in combination with mutations in the HPD region of *PAM18*. Results are summarized from experiments described in Figures 3 and 4 and the Supplemental Material. TS, temperature sensitive. Numbers in parentheses give the temperature (°C) at which the particular mutant forms colonies but grows more slowly than cells lacking the *PAM16* or *PAM18* mutation being assessed, whose phenotypes are indicated in the None column.

TABLE 1: Mutational analysis of *PAM18* and *PAM16*.

$pam18_{\Delta1-60/N140Q}$ cells were assessed to assure that the phenotypes were not due to lower levels of expression. These variants were found to be expressed at levels similar to wt (Supplemental Figure S3B). Thus, overall, the pattern of mitochondrial import defects and genetic interactions of $pam16_{L97W}$ and $pam18_{\Delta1-60}$ with the mutations affecting ATPase stimulation followed those of $pam18_{F99G/F104G}$ (Table 1).

The similarity of the synthetic genetic effects of the $pam18_{F99G/F104G}$ arm, previously proposed to affect the regulation of the ATPase stimulatory activity, and those alterations shown to affect the stability of Pam18's interaction with the translocon raised the possibility that the arm serves the role of stabilizing the Pam18:Pam16 interaction and thus Pam18's association with the translocon. Therefore we decided to test the effect of the F99G/F104G alteration in Pam18's arm on association with Pam16. Mitochondria from wt and mutant strains were lysed by the addition of Triton X-100, which also results in dissociation of the Pam18:Pam16 complex from the translocon. The resulting extracts were subjected to immunoprecipitation using Pam16-specific antibodies. As expected (D'Silva et al., 2008), Pam18 and Pam16 were efficiently coprecipitated from wt and $pam18_{\Delta1-60}$ extracts but not from extracts derived from $pam16_{L97W}$ mitochondria (Figure 4E). Coprecipitation of Pam18:Pam16 was also greatly reduced in extracts from $pam18_{F99G/F104G}$ mitochondria, indicating that these alterations in Pam18's arm affected the stability of the Pam18:Pam16 interaction. Mitochondria from $pam18_{F99G/F104G}$ were also lysed with digitonin to compare the effect of the F99/F104 alteration on the Pam18:Pam16 interaction when the heterodimer remains intact with the translocon. Compared to wt, coprecipitation of Pam18$_{F99G/F104G}$:Pam16 was again greatly reduced (Figure 4E). The levels of Tim44 were not affected by alterations in the Pam18 arm, consistent with previous results that suggest that the interaction between the Pam18:Pam16 heterodimer and Tim44 is mediated primarily by Pam16 (Kozany et al., 2004; Mokranjac et al., 2007; D'Silva et al., 2008).

Residues adjacent to the J-type domain of Pam16 are required for activity of Pam18:Pam16 heterodimer

The results of the experiments described earlier indicate that the stability of the Pam18:Pam16 heterodimer is critical for achieving a functional translocation machinery. Therefore we decided to further investigate the Pam18:Pam16 interaction. Because it was reported that Pam16 lacking its 53 N-terminal amino acids renders Pam18 incapable of stimulating Ssc1's ATPase activity (Mokranjac et al., 2006), we attempted to isolate a fragment of Pam16 that maintained Pam18 in an active form. To that end, we purified full-length Pam16 and two N-terminal truncations, Pam16$_{25-149}$ and Pam16$_{47-149}$, and then tested their effect on Pam18's stimulatory activity (Figure 5, A and B). As expected from previous reports (Frazier et al., 2004; D'Silva et al., 2005b), the addition of full-length Pam16 to Pam18 reduced Pam18's stimulatory capacity in the in vitro assay ~50% (Figure 5B). Also as expected, the heterodimer formed between Pam18 and Pam16$_{47-149}$ was inactive, similar to Pam16$_{54-149}$ (Mokranjac et al., 2006). However, Pam16$_{25-149}$ in combination with Pam18 resulted in the same level of stimulation as full-length Pam16 and Pam18. Our results are consistent with residues between 25 and 54 playing an important function in forming an active heterodimer.

Importance of the segment of Pam16 adjacent to the J-type domain in vivo

Because the in vitro experiments described earlier suggested that at least some residues between positions 25 and 54 are functionally important, we carried out an alanine scan to assess their importance

in in vivo function (Figure 5A). Changing three alanine residues at a time, we constructed eight mutants and used the plasmid-shuffling system to test for their ability to carry out Pam16 function. All mutants supported growth as well as wt PAM16 (Supplemental Figure S5). To test more rigorously the functional robustness of these Pam16 variants, we expressed them in cells expressing a Pam18 variant, Pam18$_{L150W}$. Pam18$_{L150W}$ has an alteration in the J-domain at the interface with Pam16 (Figure 1B), analogous to the L97W mutation of Pam16 used in the experiments described earlier (D'Silva et al., 2005b, 2008). However, the growth defect of $pam18_{L150W}$ cells is slightly less severe than that of $pam16_{L97W}$, as they grow nearly as well as wt cells at 34°C (D'Silva et al., 2008). Again we used the plasmid-shuffling technique to assess synthetic genetic interactions. Six of the triple-alanine PAM16 mutants showed no synthetic growth defect with $pam18_{L150W}$ (Figure 5C). On the other hand, those having substitutions at positions 48–50 ($pam16_{48-50AAA}$) and 51–53 ($pam16_{51-53AAA}$) showed severe growth defects in combination with $pam18_{L150W}$ (Figure 5C). Although $pam16_{48-50AAA}$ $pam18_{L150W}$ cells could form colonies at 23°C, $pam16_{51-53AAA}$ and $pam18_{L150W}$ were synthetically lethal, indicating the functional importance of this interval. When the triple-alanine mutations were combined with the $pam16_{L97W}$ substitution, similar results were observed (Figure 5D). Neither $pam16_{L97W/48-50AAA}$ nor $pam16_{L97W/51-53AAA}$ was able to rescue growth on 5-FOA plates, whereas the other triple-alanine mutants containing the L97W alteration grew like the $pam16_{L97W}$ single mutant (Figure 5D). To test the importance of these individual residues, mutations were made to create single-alanine substitutions at positions G48, E49, Y50, G51, G52, and I53. Each mutant was then tested in the $pam18_{L150W}$ genetic background. Most of the genetic interactions were relatively minor (Figure 5E). However, $pam16_{I53A}$ was synthetically lethal with $pam18_{L150W}$, indicating the particular importance of this residue.

Comparison between the Pam18 arm and the Pam16 region adjacent to the J-type domain

The synthetic genetic interactions of mutations affecting the region of Pam16 immediately N-terminal to the J-like domain with the L150W and L97W alterations of Pam18 and Pam16, respectively, raises the possibility that this region may play a role in the Pam16:Pam18 interaction. To compare the effect of alterations in this region of Pam16 with the analogous region of Pam18 that forms the arm that wraps around helix III of Pam16's J-like domain (Figure 5F), we examined the synthetic genetic interactions between the PAM16 mutants ($pam16_{48-50AAA}$ and $pam16_{51-53AAA}$) and the PAM18 mutants in the HPD region, which have altered stimulation of Hsp70 ATPase activity. The effects on growth were milder than those seen with $pam18_{F99G/F104G}$; however, the pattern of genetic interactions was the same (Table 1 and Supplemental Figure S6). The Pam16$_{51-53AAA}$ alteration was more severe, showing temperature-sensitive phenotypes when combined with N140Q, S147G, or P142G. $pam16_{48-50AAA}$ cells, on the other hand, grew like wild type when combined with all HPD alterations except for $pam16_{48-50AAA}$ $pam18_{P142G}$ cells, which were slightly temperature sensitive at 37°C. This pattern of genetic interactions mirrors those seen with alterations in the Pam18 arm, as well as alterations that disrupt the stability of the Pam18:Pam16 heterodimer with the translocon (Table 1).

DISCUSSION

The experiments reported here were designed to test the idea that modulation of the interface between Pam18 and Pam16 via the Pam18 arm plays a critical regulatory role, causing cycling between
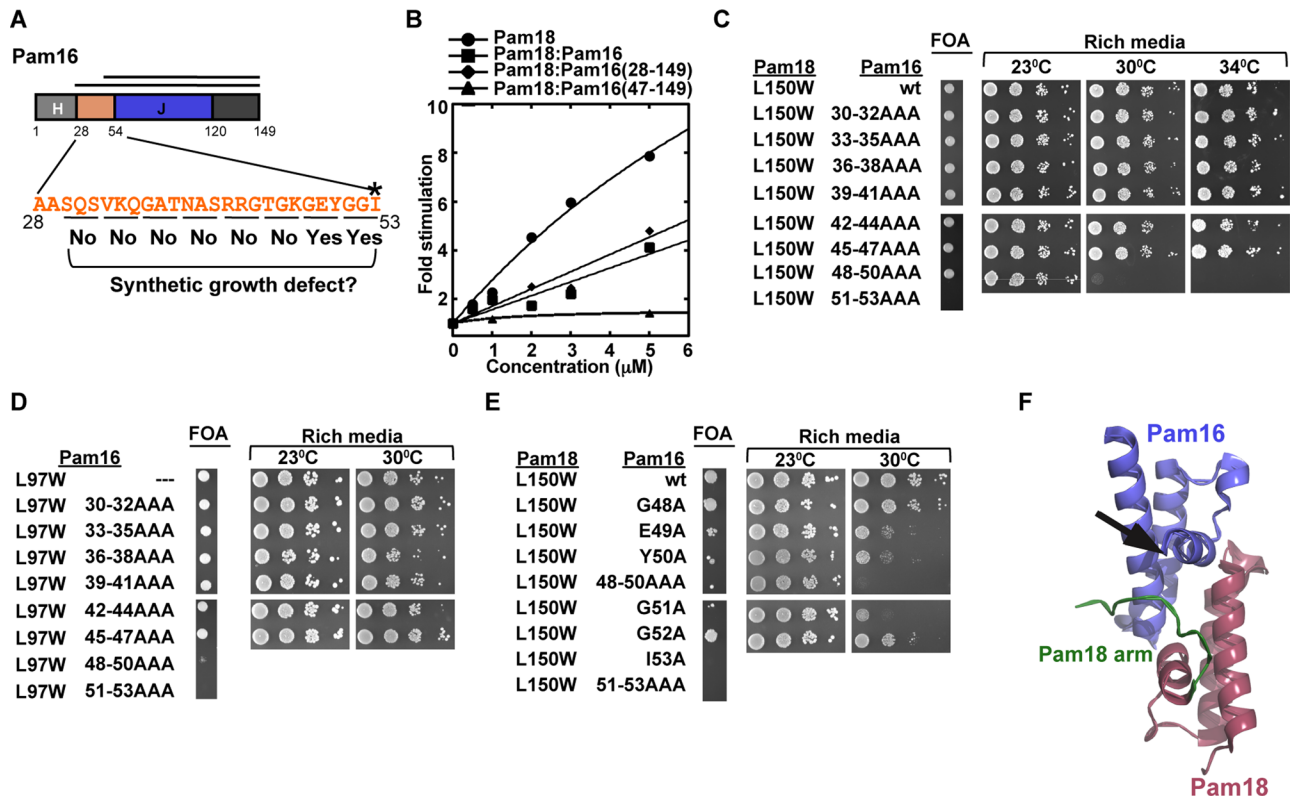
FIGURE 5: Analysis of Pam16 region adjacent to the "J-like" domain. (A) Domain organization of Pam16, with the regions of study highlighted as shown. The solid lines denote the protein truncations used in in vitro assays of Ssc1 ATPase stimulation with $Pam16_{25-149}$:Pam18 and $Pam16_{47-149}$:Pam18. The sequence of the region subjected to alanine scanning mutagenesis is shown, with the three residues altered in each mutant underlined. The presence (YES) or absence (NO) of synthetic growth defects, as shown in C and D, is indicated. I53, the individual residue showing the most extreme synthetic defects when analyzed as single–amino acid variants (E), is indicated by an asterisk. (B) Stimulation of Ssc1 ATPase activity by the Pam18:Pam16 heterodimer, under single-turnover conditions. Ssc1:[α-^{32}P]ATP complex (0.2 μM) was mixed with Pam18, alone or complexed with Pam16 proteins, at the indicated concentrations and incubated at 25°C for various times. The rate constants for ATP hydrolysis were determined as described in *Materials and Methods* and are plotted here as the fold stimulation over the basal rate determined in the absence of any J proteins versus the concentration of Pam18:Pam16. The data are fitted to a hyperbolic curve function. (C–E) Effect on growth of mutations in *PAM16* alone or in combination with other mutations in *PAM18* or *PAM16*. Strains expressing the indicated *PAM16* and *PAM18* genes were plated onto 5-FOA media and incubated at 23°C for 4 d. Strains recovered from plating on 5-FOA were then spotted in 10-fold serial dilutions onto rich glucose-based media and incubated for 2 d (30 and 34°C) or 4 d (23°C). (F) Alternative view of the structure of Pam18 (aa 99–168, pink) complexed with Pam16 (aa 54–119, blue) depicted in Figure 1B (Mokranjac *et al.*, 2006; PDB ID 2GUZ). The arm of Pam18 (green) wraps around helix III of Pam16. The arrow denotes the N-terminal residue of the Pam16 fragment and where a symmetrical region of Pam16 might interact with helix III of Pam18.

active and inactive conformations for Hsp70 ATPase stimulation. The results of our experiments provide no support for this hypothesis. Instead, our results reveal a correlation between the stability of the association of Pam18 with the translocon and a requirement for robust ATPase stimulatory capacity, suggesting a critical role of the arm of Pam18 in maintaining its association with the translocon.

Pam18's minimal ATPase stimulatory activity requirement

Our analysis revealed that decreases in ATPase stimulation of Hsp70 in the mitochondrial import system of 10-fold or more are well tolerated. Likely this robustness is at least in part attributable to the close proximity, and thus high local concentration, of Pam18 and Ssc1 at the translocon. In most instances, J-proteins and their partner Hsp70s function in solution and thus at lower effective concentrations. Perhaps there is some environmental situation that requires such high ATPase stimulatory activity, but clearly under typical labo-

ratory conditions the demand for ATPase stimulatory activity is much lower than what is available.

Pam16 residues important for robust stimulatory activity of Pam18:Pam16 heterodimer

A heterodimer between the J-type domain of Pam16 (residues 47–149) and Pam18 has negligible ATPase stimulatory activity. Our investigation into the sequence requirements of Pam16 needed to render the heterodimer fully active revealed that the N-terminal 24 amino acids are dispensable. However, residues between 25 and 54, the beginning of the core J-type domain, are critical for full stimulatory capacity of the heterodimer. These critical Pam16 residues are missing from the Pam18:Pam16 structure, having T54 as the N-terminal residue (Mokranjac *et al.*, 2006). The heterodimer structure does include the 11 amino acids immediately N-terminal of the Pam18 J-domain. These residues wrap around $Pam16_{54-119}$,

forming an "arm." It is tempting to speculate that the analogous sequences in Pam16 wrap around Pam18, also forming an arm, thus generating a symmetrical structure (Figure 5F). The inactivity of the heterodimer formed by the smaller Pam16 fragment may well reflect a requirement for Pam16 sequences analogous to those of the Pam18 arm.

Although single-alanine substitutions adjacent to the J-type domains in both Pam18 and Pam16 have little if any effect on growth, the arm region of Pam18 is arguably the more important of the two. Double-alanine substitution of positions 99 and 104 of Pam18 had severe temperature-sensitive affects on growth, whereas none of the triple-alanine substitutions of Pam16 caused obvious growth defects. In addition, the synthetic genetic interactions were more severe for alterations in the Pam18 arm when combined with alterations that affect ATPase stimulatory ability (Table 1) or with alterations that disrupt the heterodimer interface (Figure 5). However, it should be pointed out that design of mutagenesis studies of the Pam16 region is limited by the lack of availability of structural information.

Role of the Pam18 arm—regulation or stability?

An appealing hypothesis put forth previously and generally accepted (Frazier *et al.*, 2004; Mokranjac and Neupert, 2005, 2010; Mokranjac *et al.*, 2006; Neupert and Herrmann, 2007; van der Laan *et al.*, 2010; Endo *et al.*, 2011) purports that the interaction between Pam18 and Pam16 serves to regulate Pam18's Hsp70 stimulatory ability, with the arm region of Pam18 playing a critical role in this process. According to this hypothesis, the sequestering of important residues of Pam18's J-domain within the heterodimer act as an on/off switch. One of the major pieces of evidence that has been given in support of this model is the fact that the heterodimer having no sequence N-terminal of the Pam16 J-type domain is inactive and thus represents the "off" conformation. Although this explanation is possible, it seems as likely, if not more so, that this complex is simply inactive because it lacks important sequences of Pam16. On the basis of the results reported here, the residues immediately N-terminal to Pam16's J-type domain are likely candidates, as discussed earlier, as they are necessary for the ability of the Pam18:Pam16 heterodimer to have any measurable stimulatory activity.

Another argument put forth for the idea that the interaction surface between Pam18 and Pam16 serves a regulatory role is the fact that Pam18's ATPase stimulatory activity is reduced to ~50% upon formation of a heterodimer with Pam16 (Figure 5B; Li *et al.*, 2004; Chacinska *et al.*, 2005). However, on the basis of the resilience of the import process to reduction in Pam18's stimulatory capacity, we think that this modest reduction has little or no functional effect because more severe reductions in activity caused by alterations near the HPD motif are very well tolerated. The modest 50% reduction caused by Pam18:Pam16 heterodimer formation may simply be an inconsequential effect of slight conformational differences between the less stable Pam18 homodimer conformation and the more stable Pam18:Pam16 heterodimer (D'Silva *et al.*, 2005b).

Additional evidence against a regulatory role of heterodimer conformation comes from analysis of the mutations that affect residues in and around the critical HPD motif that affect the ability of Pam18 to stimulate Hsp70's ATPase activity. A corollary of the argument that the arm of Pam18 is important for inhibition of the ATPase stimulatory activity of Pam18 is that lowering this activity might be advantageous and raising it would be deleterious when the arm is disrupted. However, the results reported here demonstrate that the opposite is the case. Most compelling is the partial suppression of the F99G/F104G mutations causing alterations in

Pam18's arm, which were proposed to cause defects in regulation of Pam18's activity, by K144R, a mutation resulting in a more potent stimulatory activity. Consistent with this result, we also found that reduction of ATPase stimulatory ability by alterations such as N140Q, P142G, and S147G, although well tolerated in an otherwise wt background, were deleterious in the presence of alterations in the arm.

If the interaction between the J-type domains and adjacent sequences do not play a regulatory role, what is the function of this interaction? Our data are consistent with the idea that both play a role in stabilizing the interaction between the two proteins and thus the interaction of Pam18 at the translocon. Mutations causing alterations in either of these regions have deleterious effects when combined with others that reduce the affinity of Pam18 and Pam16, including the IMS domain of Pam18. In addition, mutations causing alterations in these regions display negative synthetic genetic interactions with alterations in and around the HPD motif that are critical for Pam18's stimulatory activity. These results are consistent with the hypothesis that the stability of association with the translocon is a primary role of the interaction between the J-type domains and associated sequences.

Perspectives

We emphasize that, although there is no experimental evidence that supports regulation of Pam18's ATPase stimulatory capacity, the idea that mechanisms exist to avoid a futile cycle of ATP hydrolysis by Hsp70 remains an appealing one because they would increase the efficiency of the import process. Modes of regulation other than altering contacts between the J-type domains of Pam16 and Pam18 can be envisioned. Because both Ssc1 and Pam18 are tethered to the translocon, a conformational change of the translocon itself or associated proteins may drive such regulation. Tim44 is a particularly appealing candidate for transmission of such regulation, as it is the site of interaction of Hsp70 and likely Pam16 (Kozany *et al.*, 2004; Mokranjac *et al.*, 2007; D'Silva *et al.*, 2008) as well. By this means, simply changes in the location in space of the Pam18 J-domain, rather than its conformation, could be a means of regulation. This model of regulation, as well as others, await experimental validation.

MATERIALS AND METHODS

Yeast strains, plasmids, and genetic methods

All mutants of *PAM18* and *PAM16* were constructed by site-directed mutagenesis using the QuikChange protocol (Stratagene, La Jolla, CA). The presence of the expected mutations was verified by sequencing. All in vivo experiments were carried out in the W303 genetic background in derivatives of PJ53 (James *et al.*, 1997). Yeast strains deleted for *PAM18* or *PAM16* carried the wt genes on pRS316, a plasmid that also encodes the URA3 gene, as described previously (D'Silva *et al.*, 2003, 2005b). Double-deletion strains were created by mating the single-deletion haploids, sporulating the resulting diploids, and dissecting tetrads to isolate the desired haploids. The centromeric plasmids pRS315 and pRS314 encoding Pam18 and Pam16 variants, respectively, were transformed into haploid yeast strains, and transformants were then plated on media containing 5-FOA to select for those cells that lost the plasmid carrying the wt genes.

Protein expression and purification

Wild-type and mutant *PAM16* and *PAM18* containing six histidine codons at the 3' or 5' end, respectively, were cloned into the pET3a plasmid to facilitate protein purification, as described previously

(D'Silva *et al.*, 2005a, 2008). Proteins were overexpressed in *Escherichia coli* strain C41 cells (Miroux and Walker, 1996) and grown at 37°C to an OD$_{600}$ of 0.6 in medium containing 100 mg/l ampicillin. Protein expression was induced by the addition of 1 mM isopropyl β-D-1-thiogalactopyranoside (IPTG) and incubated at 25°C for 5–7 h. Protein purification was then carried out using batch affinity chromatography, as described previously (D'Silva *et al.*, 2008). The proteins were eluted with 500 mM imidazole and dialyzed at 4°C against 20 mM Tris buffer, pH 8.0, 0.1 M KCl, 10% glycerol, and 0.2% Triton X-100. Protein aliquots were frozen in liquid nitrogen and stored at −80°C.

To facilitate Hsp70 purification, *SSC1* containing six histidine codons at the C-terminus was cloned into the *E. coli* expression vector pDuet, and the protein was overexpressed in BL21(DE3) cells at 30°C to an OD$_{600}$ of 0.6. Protein expression was induced by adding 0.5 mM IPTG and further incubating at 25°C for 5–7 h. Cells were harvested and resuspended in buffer A (20 mM Tris, pH 8.0, 150 mM KCl, 10% glycerol, 20 mM imidazole, 0.1% Triton X-100, 1 mM ATP, and 10 mM MgCl$_2$) containing EDTA-free protease inhibitors (Roche Diagnostics, Indianapolis, IN). Cells were lysed by two passes through the French press and centrifuged at 12,000 × *g* for 30 min at 4°C. The clarified supernatant was then loaded onto a nickel-nitriloacetic acid histidine-bind resin column (Novagen, Gibbstown, NJ) and washed with buffer A. Proteins were eluted using a 20–500 mM imidazole gradient (20 ml total). Fractions showing ≥95% purity were pooled and dialysed in 25 mM 4-(2-hydroxyethyl)-1-piperazineethanesulfonic acid (HEPES), pH 7.4, 100 mM KCl, and 10% glycerol at 4°C. There were no differences observed between Ssc1 purified from *E. coli* and yeast, which was carried out as described previously (Liu *et al.*, 2001; D'Silva *et al.*, 2008; Schiller *et al.*, 2008).

Glutathione *S*-transferase–tagged Mge1 cloned into the pGEX-KT expression vector was purified as described previously (Miao *et al.*, 1997). All protein concentrations were determined using the Bradford assay, with bovine serum albumin as a standard.

ATPase assay

All ATPase assays were performed using V459F Ssc1 to measure Hsp70 stimulation caused by J-domain binding to the ATPase domain only. Single-turnover ATPase assays were performed exactly as described previously (D'Silva *et al.*, 2003). The percentage of hydrolysis at the zero time point (~25%) was subtracted from all time points for a given reaction. The first-order rate constant was calculated from a single-exponential fit of the fraction hydrolysis versus time. For steady-state assays, 20-μl reactions were initiated by the addition of [α-^{32}P]ATP (3000 Ci/mmol; PerkinElmer, Waltham, MA) to buffer (25 mM HEPES-KOH, pH 7.4, 100 mM KCl, and 11 mM Mg(OAc)$_2$) containing Ssc1, Mge1, and Pam18/Pam16. All reactions were carried out at 25°C, quenched at various times with 4 M formic acid, 2 M LiCl, and 36 mM ATP, and spotted onto polyethyleneimine-cellulose TLC plates. Plates were developed in 1 M formic acid and 0.5 M LiCl and then analyzed by autoradiography using a PhosphorImager screen (Molecular Dynamics, Sunnyvale, CA) and ImageQuant software (GE Healthcare, Piscataway, NJ). The initial rate was calculated from a linear fit of product formation taken from the first 20% of the reaction.

Coimmunoprecipitation assay

Purification of mitochondria, affinity purification of antibody against Pam16, and cross-linking of the purified antibody to protein A using dimethylpimelimidate dihydrochloride were all carried out as described previously (Liu *et al.*, 2003). To analyze the Pam18:Pam16 interaction where the Tim23 translocon and import motor are intact, 220–300 μg of wt or mutant mitochondria were lysed in coimmunoprecipitation (coIP) buffer (20 mM Tris, pH 7.5, 80 mM KCl, 5 mM EDTA, and 10% glycerol) containing 1 mM phenylmethylsulfonyl fluoride and 1% digitonin. Samples were incubated on ice for 40 min with gentle vortexing at 10-min intervals. Lysates were then centrifuged at 14,000 rpm for 15 min at 4°C, and the supernatant was incubated with 25 μl (bed volume) of beads cross-linked to Pam16 antibody for 1–2 h at 4°C. The beads were washed once with coIP buffer containing 0.1% digitonin and twice with coIP buffer without digitonin. Samples were then subjected to SDS–PAGE, followed by immunoblot analysis. To analyze the Pam18:Pam16 interaction where the heterodimer is separated from the translocon, 1% Triton X-100 was used instead of digitonin.

Miscellaneous

All immunoblot analysis was carried out using the Enhanced Chemiluminescence system (GE Healthcare) according to the manufacturer's suggestion, by using polyclonal antibodies specific for Pam16 (D'Silva *et al.*, 2005b), Pam18 (D'Silva *et al.*, 2003), and Tim44 (Liu *et al.*, 2001). Complete synthetic media lacking specific amino acids or containing 5-FOA were prepared as described (Sikorski and Boeke, 1991). All other chemicals used were reagent grade. All results shown are representative of experiments repeated at least three times.

REFERENCES

Bukau B, Weissman J, Horwich A (2006). Molecular chaperones and protein quality control. Cell 125, 443–451.

Chacinska A *et al.* (2005). Mitochondrial presequence translocase: switching between tom tethering and motor recruitment involves Tim21 and Tim17. Cell 120, 817–829.

Craig EA, Huang P, Aron R, Andrew A (2006). The diverse roles of J-proteins, the obligate Hsp70 co-chaperone. Rev Physiol Biochem Pharmacol 156, 1–21.

D'Silva P, Marszalek J, Craig EA (2005a). An essential connection: link between Hsp70's domains at last. Mol Cell 20, 493–494.

D'Silva PD, Schilke B, Walter W, Andrew A, Craig EA (2003). J protein cochaperone of the mitochondrial inner membrane required for protein import into the mitochondrial matrix. Proc Natl Acad Sci USA 100, 13839–13844.

D'Silva PR, Schilke B, Hayashi M, Craig EA (2008). Interaction of the J-protein heterodimer Pam18/Pam16 of the mitochondrial import motor with the translocon of the inner membrane. Mol Biol Cell 19, 424–432.

D'Silva PR, Schilke B, Walter W, Craig EA (2005b). Role of Pam16's degenerate J domain in protein import across the mitochondrial inner membrane. Proc Natl Acad Sci USA 102, 12419–12424.

Endo T, Yamano K, Kawano S (2011). Structural insight into the mitochondrial protein import system. Biochim Biophys Acta 1808, 955–970.

Frazier AE *et al.* (2004). Pam16 has an essential role in the mitochondrial protein import motor. Nat Struct Mol Biol 11, 226–233.

Hutu DP, Guiard B, Chacinska A, Becker D, Pfanner N, Rehling P, van der Laan M (2008). Mitochondrial protein import motor: differential role of tim44 in the recruitment of Pam17 and J-complex to the presequence translocase. Mol Biol Cell 19, 2642–2649.

James P, Pfund C, Craig EA (1997). Functional specificity among Hsp70 molecular chaperones. Science 275, 387–389.

Jensen RE, Johnson AE (2001). Opening the door to mitochondrial protein import. Nat Struct Biol 8, 1008–1010.

Koehler CM (2004). New developments in mitochondrial assembly. Annu Rev Cell Dev Biol 20, 309–335.

Kozany C, Mokranjac D, Sichting M, Neupert W, Hell K (2004). The J domain-related cochaperone Tim16 is a constituent of the mitochondrial Tim23 preprotein translocase. Nat Struct Mol Biol 11, 234–241.

Laufen T, Mayer MP, Beisel C, Klostermeier D, Mogk A, Reinstein J, Bukau B (1999). Mechanism of regulation of Hsp70 chaperones by DnaJ cochaperones. Proc Natl Acad Sci USA 96, 5452–5457.

Li Y, Dudek J, Guiard B, Pfanner N, Rehling P, Voos W (2004). The presequence translocase-associated protein import motor of mitochondria-Pam16 functions in an antagonistic manner to Pam18. J Biol Chem 279, 38047–38054.

Liu Q, D'Silva P, Walter W, Marszalek J, Craig EA (2003). Regulated cycling of mitochondrial Hsp70 at the protein import channel. Science 300, 139–141.

Liu Q, Krzewska J, Liberek K, Craig EA (2001). Mitochondrial Hsp70 ssc1: role in protein folding. J Biol Chem 276, 6112–6118.

Mayer MP, Schroder H, Rudiger S, Paal K, Laufen T, Bukau B (2000). Multistep mechanism of substrate binding determines chaperone activity of Hsp70. Nat Struct Biol 7, 586–593.

Miao B, Davis JE, Craig EA (1997). Mge1 functions as a nucleotide release factor for ssc1, a mitochondrial Hsp70 of *Saccharomyces cerevisiae*. J Mol Biol 265, 541–552.

Miroux B, Walker JE (1996). Over-production of proteins in *Escherichia coli*: mutant hosts that allow synthesis of some membrane proteins and globular proteins at high levels. J Mol Biol 260, 289–298.

Mokranjac D, Berg A, Adam A, Neupert W, Hell K (2007). Association of the Tim14 Tim16 subcomplex with the Tim23 translocase is crucial for function of the mitochondrial protein import motor. J Biol Chem 282, 18037–18045.

Mokranjac D, Bourenkov G, Hell K, Neupert W, Groll M (2006). Structure and function of Tim14 and Tim16, the J and J-like components of the mitochondrial protein import motor. EMBO J 25, 4675–4685.

Mokranjac D, Neupert W (2005). Protein import into mitochondria. Biochem Soc Trans 33, 1019–1023.

Mokranjac D, Neupert W (2010). The many faces of the mitochondrial Tim23 complex. Biochim Biophys Acta 1797, 1045–1054.

Mokranjac D, Sichting M, Neupert W, Hell K (2003). Tim14, a novel key component of the import motor of the Tim23 protein translocase of mitochondria. EMBO J 22, 4945–4956.

Neupert W, Brunner M (2002). The protein import motor of mitochondria. Nat Rev Mol Cell Biol 3, 555–565.

Neupert W, Herrmann JM (2007). Translocation of proteins into mitochondria. Annu Rev Biochem 76, 723–749.

Rassow J, Maarse AC, Krainer E, Kubrich M, Muller H, Meijer M, Craig EA, Pfanner N (1994). Mitochondrial protein import: biochemical and genetic evidence for interaction of matrix Hsp70 and the inner membrane protein mim44. J Cell Biol 127, 1547–1556.

Rehling P, Brandner K, Pfanner N (2004). Mitochondrial import and the twin-pore translocase. Nat Rev Mol Cell Biol 5, 519–530.

Schiller D, Cheng YC, Liu Q, Walter W, Craig EA (2008). Residues of tim44 involved in both association with the translocon of the inner mitochondrial membrane and regulation of mitochondrial Hsp70 tethering. Mol Cell Biol 28, 4424–4433.

Schneider HC, Berthold J, Bauer MF, Dietmeier K, Guiard B, Brunner M, Neupert W (1994). Mitochondrial Hsp70/mim44 complex facilitates protein import. Nature 371, 768–774.

Sikorski RS, Boeke JD (1991). In vitro mutagenesis and plasmid shuffling: from cloned gene to mutant yeast. Methods Enzymol 194, 302–318.

Tamura Y, Harada Y, Shiota T, Yamano K, Watanabe K, Yokota M, Yamamoto H, Sesaki H, Endo T (2009). Tim23-Tim50 pair coordinates functions of translocators and motor proteins in mitochondrial protein import. J Cell Biol 184, 129–141.

Truscott KN *et al.* (2003). A J-protein is an essential subunit of the presequence translocase-associated protein import motor of mitochondria. J Cell Biol 163, 707–713.

van der Laan M, Hutu DP, Rehling P (2010). On the mechanism of preprotein import by the mitochondrial presequence translocase. Biochim Biophys Acta 1803, 732–739.

Wiedemann N, Frazier AE, Pfanner N (2004). The protein import machinery of mitochondria. J Biol Chem 279, 14473–14476.